Article

Targeting of temperate phages drives loss of type I CRISPR–Cas systems

https://doi.org/10.1038/s41586-020-1936-2

Received: 1 February 2019

Accepted: 25 November 2019

Published online: 22 January 2020

Clare Rollie[1,6*], Anne Chevallereau[1,6*], Bridget N. J. Watson[1], Te-yuan Chyou[2], Olivier Fradet[1], Isobel McLeod[1], Peter C. Fineran[3,4], Chris M. Brown[2,4], Sylvain Gandon[5] & Edze R. Westra[1*]

On infection of their host, temperate viruses that infect bacteria (bacteriophages; hereafter referred to as phages) enter either a lytic or a lysogenic cycle. The former results in lysis of bacterial cells and phage release (resulting in horizontal transmission), whereas lysogeny is characterized by the integration of the phage into the host genome, and dormancy (resulting in vertical transmission)[1]. Previous co-culture experiments using bacteria and mutants of temperate phages that are locked in the lytic cycle have shown that CRISPR–Cas systems can efficiently eliminate the invading phages[2,3]. Here we show that, when challenged with wild-type temperate phages (which can become lysogenic), type I CRISPR–Cas immune systems cannot eliminate the phages from the bacterial population. Furthermore, our data suggest that, in this context, CRISPR–Cas immune systems are maladaptive to the host, owing to the severe immunopathological effects that are brought about by imperfect matching of spacers to the integrated phage sequences (prophages). These fitness costs drive the loss of CRISPR–Cas from bacterial populations, unless the phage carries anti-CRISPR (acr) genes that suppress the immune system of the host. Using bioinformatics, we show that this imperfect targeting is likely to occur frequently in nature. These findings help to explain the patchy distribution of CRISPR–Cas immune systems within and between bacterial species, and highlight the strong selective benefits of phage-encoded acr genes for both the phage and the host under these circumstances.

CRISPR–Cas adaptive immune systems provide sequence-specific resistance against phage infections by inserting phage-derived sequences (spacers) of around 30 bp into CRISPR loci on the host genome[4]. Upon reinfection, CRISPR transcripts guide Cas proteins to destroy the matching target[5]. The uptake of new spacers is far more efficient if a pre-existing spacer has partial complementarity to the phage. This process (known as 'priming') is widespread in type I CRISPR–Cas systems, and provides protection against phage mutants that overcome host resistance by point mutation of their target sites[6,7]. However, partially matching spacers can also cause immunopathological effects when temperate phages enter the lysogenic lifecycle, during which the phage genome is integrated into that of the host and exists in a dormant state until it is induced. Lysogens (that is, bacterial cells that carry at least one prophage) are found across bacterial genera; however, their frequencies vary[8]. During lysogeny, a primed CRISPR–Cas immune system may target the partially complementary site in the prophage, causing damage to both the phage and host DNA and resulting in the induction of the SOS response[9]. However, whether and how these potentially negative effects influence the evolutionary and population dynamics of CRISPR–phage interactions remains unclear, because these processes have previously been studied only in the context of virulent phages[2,3].

Temperate phages persist despite CRISPR

To explore CRISPR–phage interactions in the context of lysogeny, we infected *Pseudomonas aeruginosa* PA14 with the temperate phage DMS3 or the virulent mutant DMS3vir (a DMS3 mutant that is locked in the lytic cycle through mutation of the c-repressor gene) and monitored bacterial and phage population dynamics for eight days. *P. aeruginosa* strain PA14 carries a type I-F CRISPR–Cas immune system, in which spacer 1 of CRISPR array 2 has an imperfect match (5 mismatches) to gene 42 of DMS3[9,10]. As previously reported[3], DMS3vir was driven extinct by wild-type bacteria at five days post-infection owing to the evolution of CRISPR-based resistance, whereas a Δ*cas7* mutant of the PA14 strain (hereafter Δ*cas7*—which lacks a functional CRISPR–Cas system—evolved surface-based resistance that allowed for phage persistence (Fig. 1a–c). By contrast, both wild-type and Δ*cas7* bacteria were unable to clear wild-type DMS3 infections (Fig. 1b), which suggests that the ability to transmit vertically (during lysogeny) is a critical determinant of the survival of temperate phages when bacteria encode CRISPR–Cas immune systems. To understand the evolutionary drivers of these population dynamics, we isolated bacterial clones from the DMS3-infected cultures at three days post-infection and quantified the proportion of lysogens and bacteria with CRISPR-based and surface-based

[1]ESI, Biosciences, University of Exeter, Penryn, UK. [2]Department of Biochemistry, University of Otago, Dunedin, New Zealand. [3]Department of Microbiology and Immunology, University of Otago, Dunedin, New Zealand. [4]Genetics Otago, University of Otago, Dunedin, New Zealand. [5]CEFE, Université de Montpellier, CNRS, EPHE, IRD, Université Paul Valéry Montpellier 3, Montpellier, France. [6]These authors contributed equally: Clare Rollie, Anne Chevallereau. *e-mail: C.Rollie@exeter.ac.uk; A.Chevallereau@exeter.ac.uk; E.R.Westra@exeter.ac.uk

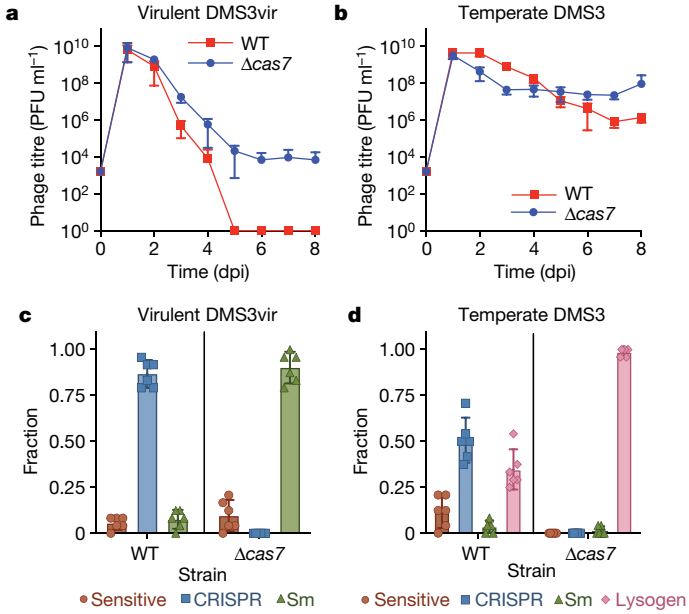


Fig. 1 | Phage persistence and evolution of resistance in the host upon infection with virulent or temperate phages. a, **b**, Phage densities over time after infection of wild-type (WT) PA14 or the Δ*cas7* mutant with DMS3vir (**a**) or DMS3 (**b**). The limit of phage detection is 200 plaque-forming units per millilitre (PFU ml^{-1}). **c**, **d**, Fraction of bacteria that evolved resistance at three days post-infection (dpi) after infection with the phages DMS3vir (**c**) or DMS3 (**d**), either through CRISPR–Cas (CRISPR), surface modification (sm) or lysogeny (lysogen). Fractions are based on 24 random clones per replicate experiment. In all panels, data are the mean of six biologically independent replicates per treatment. Error bars represent 95% confidence intervals.

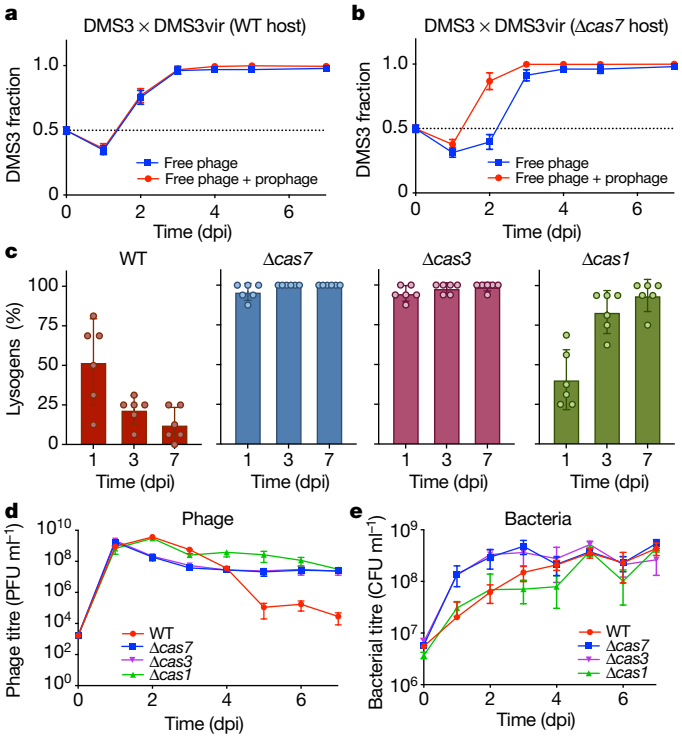


Fig. 2 | The effect of CRISPR adaptation and interference on lysogeny and phage persistence. a, **b**, Relative frequencies of DMS3 over time after infection of wild-type PA14 (**a**) or the Δ*cas7*-mutant (**b**) host with an equal mix of DMS3 and DMS3vir. Relative frequencies are shown both for the free and total (that is, including lysogens) phage population. **c**, Percentage of DMS3 lysogens in the host population at 1, 3 or 7 days post-infection of the wild-type PA14 strain, the isogenic CRISPR-interference deficient mutants Δ*cas7* and Δ*cas3*, or the isogenic CRISPR-adaptation-deficient mutant Δ*cas1*, based on 24 random clones per replicate experiment per time point. **d**, **e**, DMS3 phage (**d**) and bacterial densities (**e**) during this co-culture experiment. CFU, colony-forming unit. In all panels, data are the mean of six biologically independent replicates per treatment. Error bars represent 95% confidence intervals.

resistance. This showed that the evolution of CRISPR-based resistance was substantially reduced in wild-type populations of bacteria exposed to DMS3 compared to those exposed to DMS3vir (Fig. 1c, d); instead, many wild-type bacteria carried the DMS3 prophage (Fig. 1d), which confers phage resistance through superinfection exclusion. However, lysogeny levels were reduced in wild-type hosts compared to in the Δ*cas7* strain, which almost invariably carried the prophage (Fig. 1d).

The difference in DMS3 and DMS3vir persistence could be due to differences in the evolution of resistance in the host or to the ability of DMS3 to transmit vertically while continuously releasing free phage particles through prophage induction. To distinguish between these possibilities, we infected wild-type and Δ*cas7* strains with an equal mix of DMS3 and DMS3vir, and observed bacterial and phage population dynamics and resistance evolution similar to those that were observed during infection with the temperate phage alone (Extended Data Fig. 1). Next, we examined how the relative frequencies of DMS3 and DMS3vir changed over time (Fig. 2a, b). Initially, DMS3vir outcompetes DMS3, consistent with the idea that high densities of sensitive hosts favour horizontal transmission (the lytic replication cycle)[11]. However, at later time points, all free phage particles belong to the DMS3 phage genotype. As the host population that was experienced by the two phages was identical, this demonstrates that vertical transmission facilitates the observed persistence of DMS3. The persistence of free phages was facilitated despite the low frequencies of lysogeny in wild-type compared to Δ*cas7* bacteria (compare the blue and red lines in Fig. 2a, b, Extended Data Fig. 1c, d).

To understand why lysogen formation was depressed in wild-type bacteria compared to Δ*cas7* bacteria, we performed temporal sampling of DMS3-infected populations over seven days. This revealed that lysogeny in wild-type bacteria was already depressed at one day post-infection and continued to decline until seven days post-infection, whereas the proportion of lysogens in isogenic mutants with a defective CRISPR-interference pathway (the Δ*cas3* and Δ*cas7* mutants of PA14) was high and constant during this same period (Fig. 2c). Crucially, the proportion of DMS3 lysogens at one day post-infection was also depressed in a Δ*cas1* mutant of PA14, which is unable to acquire novel spacers (adaptation) but is proficient in detecting and destroying complementary DNA (interference). However, in this background, the proportion of lysogens increased between one and seven days post-infection to levels similar to those in the CRISPR-interference mutants (Fig. 2c). These data therefore suggest that wild-type and Δ*cas1* bacteria are partially resistant to DMS3 infection (even in the absence of spacer acquisition), which results initially in fewer lysogens and further reductions if the hosts carry the genetic machinery to acquire additional spacers.

Mismatched spacers are maladaptive

We hypothesized that the observed suppression of lysogeny in wild-type and Δ*cas1* backgrounds was dependent on the imperfect match (5 mismatches) between gene 42 of DMS3 and spacer 1 of CRISPR array 2 (refs. [9,10]). To test this, we infected a strain that lacks CRISPR array 2 (ΔCRISPR2) with DMS3 and observed that the plasmid-based expression of spacer 1 (ΔCRISPR2-sp1) led to population dynamics similar to those observed during infection of the wild-type strain (Extended Data Fig. 2a, b) and suppression of lysogeny (Extended Data Fig. 2c), whereas expression of a control non-targeting spacer (ΔCRISPR2-NT) did not.

To further corroborate the hypothesis that the suppression of lysogeny was caused by partial CRISPR–Cas resistance, we performed infections with phages that carry acr genes, which are widespread and diverse genes (currently classified into 47 families) that are encoded by a range of mobile genetic elements and that block CRISPR interference[12]. As expected, the infection of wild-type bacteria with a mutant DMS3 phage that carries *acrIF1* or *acrIF4* (both of which block the type I-F CRISPR–Cas system of PA14[13]) showed levels of lysogeny similar to those observed for interference-deficient mutants (Extended Data Fig. 3a).

Although lysogen formation was reduced in wild-type and Δ*cas1* bacteria, the concentration of free phage was actually higher during the early stages of DMS3 infection in these hosts (Fig. 2d). This effect disappeared by seven days post-infection if bacteria were unable to acquire new spacers (the Δ*cas1* strain), or inverted at four days post-infection if the bacteria had a functional CRISPR–Cas system (Fig. 2d). This also coincided with reduced bacterial densities of wild-type and Δ*cas1* populations compared to CRISPR-interference mutants during the early stages of the phage epidemic (Fig. 2e), which suggests that functional CRISPR–Cas immune systems may be maladaptive in this context. We speculated that the high DMS3 titres during early stages of infection of wild-type and Δ*cas1* bacteria (Figs. 1b, 2d), and the concurrent reduced bacterial densities, could be due to interactions between the CRISPR-interference machinery and the partially complementary prophage (autoimmunity), which can activate an SOS response[9] and which—in turn—may trigger prophage induction[14]. To test this, we isolated six independent DMS3 lysogens from wild-type, Δ*cas7* and Δ*cas1* backgrounds at one day post-infection. Growth measurements revealed considerable fitness costs of lysogeny in wild-type and Δ*cas1* backgrounds, whereas the growth of Δ*cas7* lysogens was unaffected (Fig. 3a–c). The growth of lysogens that lack spacers 1 and 2 of CRISPR 2 (Δsp1–2) or lack the entire CRISPR 2 array (ΔCRISPR2-NT) was comparable to that of Δ*cas7* lysogens (Fig. 3d, Extended Data Fig. 2c), but restoring the expression of CRISPR 2 spacer 1 (ΔCRISPR2-sp1) resulted in a reduced growth rate (Extended Data Fig. 2d), which confirms that this spacer is responsible for the reduced fitness of wild-type bacteria that carry the prophage. Competition of lysogens against bacteria with surface-based resistance confirmed a fitness cost of lysogeny in the wild-type—but not in the Δ*cas7*—background (relative fitness < 1, one-tailed Wilcoxon signed-rank and *t*-tests; wild type, degrees of freedom = 5, $P = 0.016$; Δ*cas7*, $t_5 = 3.6551$, $P = 0.99$) (Fig. 3e, f). This effect was reduced if the prophage encoded an Acr (one-tailed *t*-test; *acrIF1*, $t_5 = 16.562$; *acrIF4*, $t_5 = 14.805$ and $P < 0.0001$ in both cases) (Fig. 3e), whereas acr genes had no effect on fitness of Δ*cas7* lysogens (analysis of variance (ANOVA) $F_{2,15} = 0.205$, $P = 0.82$) (Fig. 3f).

Next, we estimated prophage induction levels in wild-type and Δ*cas7* lysogens. To this end, we pelleted bacterial cultures and washed away free phages, and then resuspended in fresh medium, and monitored bacterial densities and free phage accumulation over 25 h. Although initial cell densities were similar for all strains, the growth of wild-type cultures plateaued at a lower density than that of other backgrounds (Extended Data Fig. 3b), but wild-type cultures accumulated more phage particles compared to Δ*cas7* lysogens (Extended Data Fig. 3c)—unless the prophage carried an acr gene. Taken together, these data support the hypothesis that (unless DMS3 encodes acr genes) CRISPR–Cas causes immunopathology during vertical transmission of the phage, which triggers prophage induction and therefore explains the high free-phage titres during the early infection stage.

These immunopathological effects may select for CRISPR mechanisms that selectively target phages during their lytic cycle, as has previously been described for type III systems[15,16]. However, competition between DMS3 and DMS3vir phages showed that the main determinant of their relative fitness is the proportion of sensitive bacteria in the population[11] (two-way ANOVA, $F_{6,83} = 3.1683$, $P = 0.008$) (Extended Data Fig. 3d) and is independent of whether resistance of bacteria in the population was CRISPR-based or surface-based ($F_{1,76} = 2.8923$, $P = 0.09$)

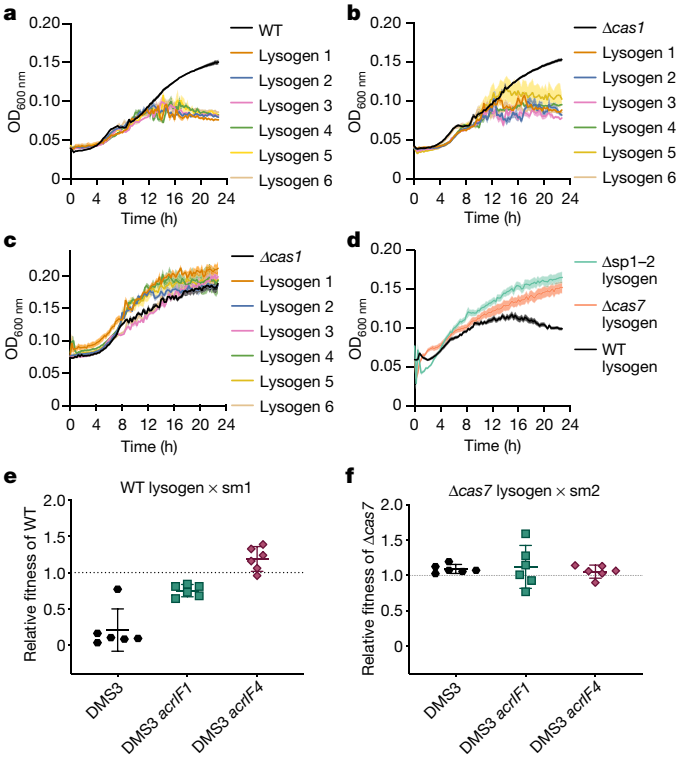


Fig. 3 | Fitness of lysogens with an active CRISPR–Cas system is reduced unless they encode acr genes. a, Twenty-four-hour growth curves of uninfected control cultures, or six independent DMS3 lysogens in wild-type PA14 (**a**), Δ*cas1* (CRISPR-adaptation-deficient) (**b**) and Δ*cas7* (CRISPR-interference-deficient) (**c**) genetic backgrounds. Lysogens were isolated from day 1 of the co-culture experiment shown in Fig. 2. Curves are the mean of six (**a**, **b**) or four (**c**) replicates and shaded areas represent s.e.m. $OD_{600\,nm}$, optical density at 600 nm. **d**, Twenty-four-hour mean growth curves of six lysogens in wild-type, Δ*cas7* and Δsp1–2 (carrying a deletion of CRISPR2 spacers 1 and 2) backgrounds isolated from six biological replicates. Each growth curve was performed in five technical replicates. Shaded areas represent s.e.m. **e**, **f**, Fitness relative to a mutant of PA14 with a surface modification (sm) of wild-type PA14 lysogens isolated one day post-infection with DMS3 (**e**) or PA14 Δ*cas7* lysogens isolated one day post-infection with DMS3 (**f**). Relative fitness was determined after one day of competition. Each point represents the average relative fitness of one independent lysogen clone measured across six biologically independent experiments. Error bars indicate 95% confidence intervals.

(Extended Data Fig. 3d). This suggests that the type I CRISPR–Cas system of *P. aeruginosa* lacks the ability to distinguish between phages that enter lytic or lysogenic cycles.

Given these opposing fitness effects of CRISPR–Cas immune systems during horizontal[2,3] and vertical transmission of DMS3 (Fig. 3), it is unclear what the net fitness effects of CRISPR–Cas systems are during temperate-phage infections. To explore this, we competed wild-type and Δ*cas7* strains in the presence of DMS3vir, DMS3, DMS3 *acrIF1* or DMS3 *acrIF4* phages and determined their relative fitness at days 1, 3 and 7. Notably, although wild-type bacteria were fitter than Δ*cas7* in the presence of the virulent phage (one-tailed Wilcoxon signed-rank test, relative fitness > 1, $P = 0.016$) (Fig. 4a), they were considerably less fit during temperate-phage infection (relative fitness < 1, $P = 0.018$) (Fig. 4a), unless the temperate phage carried acr genes (relative fitness ≠ 1, $P = 0.16$) (Fig. 4a). Therefore, in this context, acr genes not only provide a benefit to the phage during both horizontal[3,17,18] and vertical transmission of the phage (one-tailed *t*-test, relative fitness ≠ 1; *acrIF1*, $t_5 = 39.30$, $P < 0.0001$; *acrIF4*, $t_5 = 11.61$, $P < 0.0001$) (Fig. 4b) but also to the host, by preventing autoimmunity.

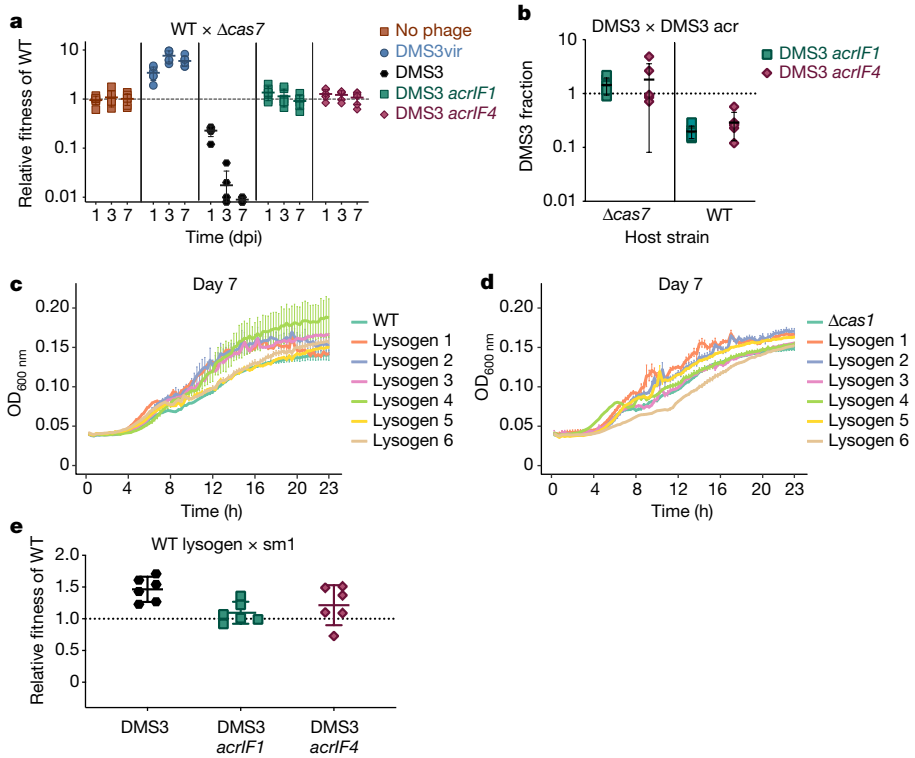


Fig. 4 | Lysogens evolve to mitigate fitness costs. a, Relative fitness of wild-type PA14 during competition with the Δ*cas7* mutant strain following infection with 10^4 PFU of DMS3, the lytic mutant DMS3vir or the anti-CRISPR-encoding mutants DMS3 *acrIF1* and DMS3 *acrIF4*. **b**, Relative fitness of DMS3 (free phages + lysogens) following three days of competition with DMS3 *acrIF1* or DMS3 *acrIF4* on either wild-type PA14 or Δ*cas7* mutant. **c**, **d**, Twenty-four-hour growth curves of uninfected control cultures, or six biologically independent DMS3 lysogens in the wild-type PA14 (**c**) or Δ*cas1* (**d**) genetic backgrounds, which were isolated from day 7 of the co-culture experiment shown in Fig. 2. Curves are the mean of six replicates and error bars represent s.e.m. **e**, Relative fitness of a DMS3 lysogen in a wild-type PA14 genetic background, isolated from day 5 of a co-culture experiment, during competition with a surface mutant. Relative fitness was calculated after one day of competition. All panels show the mean of six biologically independent replicates per treatment. Error bars represent 95% confidence intervals (**a**, **b**, **e**) or s.e.m. (**c**, **d**).

Bacteria evolve to lose CRISPR–Cas

We next monitored whether wild-type lysogens evolved to alleviate these autoimmunity costs through mutation of their immune system or the prophage. Lysogens in wild-type and adaptation-deficient Δ*cas1* backgrounds, which had reduced growth during early infection, were selected from a late stage of the infection (seven days after infection). Growth curves revealed that the negative fitness consequences of CRISPR–Cas immune systems had disappeared in these 'late' lysogens, and that these bacteria now had growth rates comparable those of ancestral hosts that lack the prophage (Fig. 4c, d; compare to Fig. 3a,b). A competition experiment confirmed this finding, which shows that late lysogens in a wild-type background were fitter than a surface mutant (one-tailed *t*-test, relative fitness > 1, $t_5 = 5.985$, $P < 0.001$) (Fig. 4e), and the presence of acr genes in the prophage no longer increased the fitness of the host (one-tailed *t*-test, *acrIF1*, $t_5 = -5.5085$, $P = 1.00$; *acrIF4*, $t_5 = -2.0395$, $P = 0.95$) (Fig. 4e, compare to Fig. 3e).

To understand the mechanistic basis for this alleviation in fitness costs, we performed PCR analyses of the CRISPR loci of six independent lysogens in wild-type, Δ*cas1* and Δ*cas7* backgrounds, isolated from early or late time points after infection. Both CRISPR loci (1 and 2) amplified as expected in early lysogens (Extended Data Fig. 4a); however, amplification failed in many late lysogens in wild-type and Δ*cas1* backgrounds (Extended Data Fig. 4a, negative PCR indicated by red frame), which suggests that the CRISPR–Cas locus was lost in these clones. Whole-genome sequencing of late lysogens revealed large genomic deletions (between about 50 and 230 kb), associated with prophage integration, that encompassed the entire CRISPR–Cas locus—but contained no essential gene[19]—in wild-type and Δ*cas1* backgrounds, whereas the genome remained intact in Δ*cas7* late lysogens (Extended Data Fig. 4c–e, Extended Data Table 1). This loss of the CRISPR–Cas locus was clearly driven by the immunopathological effects of CRISPR 2 spacer 1, as the locus was maintained in lysogens that lack CRISPR 2 (ΔCRISPR2) but was lost when expression of spacer 1 was restored (ΔCRISPR2-sp1) (Extended Data Fig. 2b). The loss of CRISPR–Cas was also avoided when wild-type bacteria were lysogenized by DMS3 that carry acr genes (Extended Data Fig. 4a).

Generality of the empirical data

Collectively, these data show that temperate-phage infection can drive the rapid loss of CRISPR–Cas immune systems from bacterial genomes owing to immunopathological effects that manifest during vertical transmission. To generalize our findings beyond phage DMS3 (which belongs to the *Caudovirales*), we introduced a priming spacer with one mismatch against the Pf5 prophage (which belongs to the *Inoviridae*) that is naturally present in the genome of wild-type PA14[20]. Expression of a Pf5-priming spacer caused reduced growth of the wild-type PA14 strain and strong selection for bacteria that carry deletions in their CRISPR–Cas immune system (Extended Data Fig. 5). These observations therefore suggest that immunopathological effects generally drive selection for CRISPR loss, whenever hosts carry spacers primed against their prophage. Indeed, when we formalized these ideas in a theoretical framework, we recovered population and evolutionary dynamics very similar to those observed in our experiments (Extended Data Fig. 6; a detailed description of the model is provided in the Supplementary Information).

Crucially, in nature, priming is thought to be frequent owing to the relaxed sequence-identity requirements for triggering this pathway: up to 13 mismatches between a pre-existing spacer and the target are tolerated[7]. Indeed, analysis of the spacers from more than 170,000 bacterial genomes and a dataset of about 20,000 prophages[21] revealed that pre-existing spacers with perfect (no mismatches) or imperfect (1–5 mismatches) targets to temperate phages are common within genera (Extended Data Fig. 7; further information is in the Supplementary Information). On average, 49% of all prophages were targeted by priming spacers carried by bacteria within the same genera as the lysogen (Extended Data Fig. 7c). If mismatched spacers generally cause residual DNA cleavage activity by the CRISPR immune system, they would be expected to cause immunopathological effects similar to those observed for the *P. aeruginosa*–DMS3 interaction. Indeed, when all complete *P. aeruginosa* genomes were assessed, we observed a significant enrichment for an increase in the frequency of acr genes when self-targeting spacers matched prophages (Extended Data Fig. 8), which is consistent with the idea that these spacers cause immunopathological effects. Together, these bioinformatic analyses suggest that—in nature—the maladaptive effects of CRISPR–Cas against temperate phages are likely to be common.

In natural ecosystems, bacteria are frequently exposed to both temperate and virulent phages, and the latter may superinfect the lysogens. To further generalize our findings, we explored whether these superinfections would be likely to change the observed population and evolutionary dynamics. We found that a mixed infection of wild-type PA14 with the temperate phage DMS3 and the virulent phage LMA2 (which can superinfect DMS3 lysogens) resulted in rates of lysogenization similar to those with the temperate phage alone (Extended Data Fig. 9d, e) and high fitness costs of CRISPR–Cas (Extended Data Fig. 9g), which drive the evolutionary loss of the immune systems (Extended Data Fig. 9f). Our theoretical model recovered similar dynamics, independent of whether CRISPR-based resistance evolves against only one (as in our experiment) or against both phages (Extended Data Fig. 9h–o).

Discussion

The observations that approximately 60% of all bacterial genotypes lack CRISPR–Cas systems, and that closely related strains differ in whether they encode cas genes, suggest that these systems are frequently gained and lost from bacterial genomes[22]. Although phage infection is typically assumed to be an important selective force for the maintenance of CRISPR–Cas immune systems, this work reveals their rapid loss when exposed to a temperate phage, as a result of the immunopathological effects that occur when the CRISPR immune system is primed against this phage. Some CRISPR–Cas immune systems may mitigate some of these autoimmunity costs by limiting the spacer acquisition from, and cleavage of, transcriptionally silent elements[15,23]. However, CRISPR-based autoimmunity has frequently been reported[24–27], and the high frequencies at which primed self-targeting interactions occur suggests that this is probably a major driver of the evolutionary loss of CRISPR systems in nature.

Online content

Any methods, additional references, Nature Research reporting summaries, source data, extended data, supplementary information, acknowledgements, peer review information; details of author contributions and competing interests; and statements of data and code availability are available at https://doi.org/10.1038/s41586-020-1936-2.

1. Stewart, F. M. & Levin, B. R. The population biology of bacterial viruses: why be temperate. *Theor. Popul. Biol.* **26**, 93–117 (1984).
2. Westra, E. R. et al. Parasite exposure drives selective evolution of constitutive versus inducible defense. *Curr. Biol.* **25**, 1043–1049 (2015).
3. van Houte, S. et al. The diversity-generating benefits of a prokaryotic adaptive immune system. *Nature* **532**, 385–388 (2016).
4. Barrangou, R. et al. CRISPR provides acquired resistance against viruses in prokaryotes. *Science* **315**, 1709–1712 (2007).
5. Garneau, J. E. et al. The CRISPR/Cas bacterial immune system cleaves bacteriophage and plasmid DNA. *Nature* **468**, 67–71 (2010).
6. Datsenko, K. A. et al. Molecular memory of prior infections activates the CRISPR/Cas adaptive bacterial immunity system. *Nat. Commun.* **3**, 945 (2012).
7. Fineran, P. C. et al. Degenerate target sites mediate rapid primed CRISPR adaptation. *Proc. Natl Acad. Sci. USA* **111**, E1629–E1638 (2014).
8. Howard-Varona, C., Hargreaves, K. R., Abedon, S. T. & Sullivan, M. B. Lysogeny in nature: mechanisms, impact and ecology of temperate phages. *ISME J.* **11**, 1511–1520 (2017).
9. Heussler, G. E. et al. Clustered regularly interspaced short palindromic repeat-dependent, biofilm-specific death of *Pseudomonas aeruginosa* mediated by increased expression of phage-related genes. *mBio* **6**, e00129-15 (2015).
10. Zegans, M. E. et al. Interaction between bacteriophage DMS3 and host CRISPR region inhibits group behaviors of *Pseudomonas aeruginosa*. *J. Bacteriol.* **191**, 210–219 (2009).
11. Berngruber, T. W., Froissart, R., Choisy, M. & Gandon, S. Evolution of virulence in emerging epidemics. *PLoS Pathog.* **9**, e1003209 (2013).
12. Trasanidou, D. et al. Keeping CRISPR in check: diverse mechanisms of phage-encoded anti-CRISPRS. *FEMS Microbiol. Lett.* **366**, fnz098 (2019).
13. Bondy-Denomy, J. et al. Multiple mechanisms for CRISPR–Cas inhibition by anti-CRISPR proteins. *Nature* **526**, 136–139 (2015).
14. Little, J. W. & Michalowski, C. B. Stability and instability in the lysogenic state of phage lambda. *J. Bacteriol.* **192**, 6064–6076 (2010).
15. Goldberg, G. W., Jiang, W., Bikard, D. & Marraffini, L. A. Conditional tolerance of temperate phages via transcription-dependent CRISPR–Cas targeting. *Nature* **514**, 633–637 (2014).
16. Samai, P. et al. Co-transcriptional DNA and RNA cleavage during type III CRISPR–Cas immunity. *Cell* **161**, 1164–1174 (2015).
17. Landsberger, M. et al. Anti-CRISPR phages cooperate to overcome CRISPR–Cas immunity. *Cell* **174**, 908–916 (2018).
18. Borges, A. L. et al. Bacteriophage cooperation suppresses CRISPR–Cas3 and Cas9 immunity. *Cell* **174**, 917–925 (2018).
19. Poulsen, B. E. et al. Defining the core essential genome of *Pseudomonas aeruginosa*. *Proc. Natl Acad. Sci. USA* **116**, 10072–10080 (2019).
20. Mooij, M. J. et al. Characterization of the integrated filamentous phage Pf5 and its involvement in small-colony formation. *Microbiology* **153**, 1790–1798 (2007).
21. Zhou, Y., Liang, Y., Lynch, K. H., Dennis, J. J. & Wishart, D. S. PHAST: a fast phage search tool. *Nucleic Acids Res.* **39**, W347–W52 (2011).
22. Makarova, K. S. et al. An updated evolutionary classification of CRISPR–Cas systems. *Nat. Rev. Microbiol.* **13**, 722–736 (2015).
23. Levy, A. et al. CRISPR adaptation biases explain preference for acquisition of foreign DNA. *Nature* **520**, 505–510 (2015).
24. Stern, A., Keren, L., Wurtzel, O., Amitai, G. & Sorek, R. Self-targeting by CRISPR: gene regulation or autoimmunity? *Trends Genet.* **26**, 335–340 (2010).
25. Vercoe, R. B. et al. Cytotoxic chromosomal targeting by CRISPR/Cas systems can reshape bacterial genomes and expel or remodel pathogenicity islands. *PLoS Genet.* **9**, e1003454 (2013).
26. Jiang, W. et al. Dealing with the evolutionary downside of CRISPR immunity: bacteria and beneficial plasmids. *PLoS Genet.* **9**, e1003844 (2013).
27. Goldberg, G. W. et al. Incomplete prophage tolerance by type III-A CRISPR–Cas systems reduces the fitness of lysogenic hosts. *Nat. Commun.* **9**, 61 (2018).

Publisher's note Springer Nature remains neutral with regard to jurisdictional claims in published maps and institutional affiliations.

© The Author(s), under exclusive licence to Springer Nature Limited 2020

Methods

No statistical methods were used to predetermine sample size. The experiments were not randomized and investigators were not blinded to allocation during experiments and outcome assessment.

Bacterial strains and viruses

P. aeruginosa UCBPP-PA14 (referred to as wild type) and *P. aeruginosa* UCBPP-PA14 *csy3::lacZ* (referred to as Δ*cas7*) were used in all experiments, and have previously been described[28]. The surface mutant *Tn::pilA* (which lacks a pilus, and is referred to as sm2) has previously been described[29] and was used in competition experiments with a bacteriophage insensitive mutant (BIM) with two additional acquired spacers over those present in the wild-type strain, as previously described[2].

Lysogens in wild-type or CRISPR-mutant backgrounds used in growth curves, fitness and induction experiments were generated in this study; the presence of a prophage was confirmed by PCR. PA14 strains Δ*cas3*, Δ*cas1*, ΔCRISPR2 and CRISPR2 Δsp1–2 identified, respectively, as SMC4268, SMC4277 and SMC3895 and SMC4707, have previously been described[10,28].

Phage amplifications were carried out on *P. aeruginosa* UCBPP-PA14 *csy3::lacZ*. DMS3 and the obligate lytic variant DMS3vir have previously been described[30]. DMS3 *acrIF1* and DMS3 *acrIF4* phages were generated in this study following a method for hybrid phage construction detailed in a previous study[17]. DMS3vir *acrIF1* was used in downstream analyses and has previously been described[3]. A virulent phage capable of infecting DMS3 lysogens (LMA2, which has previously been described[31]) was used in co-culture experiments.

All bacterial strains were grown at 37 °C in LB broth or M9 medium (22 mM Na_2HPO_4; 22 mM KH_2PO_4; 8.6 mM NaCl; 20 mM NH_4Cl; 1 mM $MgSO_4$; and 0.1 mM $CaCl_2$) supplemented with 0.2% glucose. When appropriate, medium was further supplemented with gentamycin (50 mg/ml) and arabinose (1% w/v).

Evolution experiments

To monitor the evolution of bacterial resistance in response to phage infection and the associated bacterial and phage population dynamics, microcosms with 6 ml of M9 medium supplemented with 0.2% glucose were inoculated with approximately 10^6 CFU bacteria from fresh overnight cultures of the corresponding bacterial strains. These cultures were infected with 10^4 PFU of DMS3vir, DMS3, DMS3 *acrIF* or LMA2 phages, followed by incubation at 37 °C and shaking at 180 rpm. Cultures were transferred 1:100 into fresh medium every 24 h for 5–8 days. All experiments were performed in six independent replicates.

Determination of resistance phenotypes

Resistance phenotypes were determined at day 3 or day 7 by streaking individual colonies (24 randomly picked per replicate) through DMS3vir and anti-CRISPR phage DMS3vir *acrIF1*. Surface modification was confirmed by colony morphology, broad-range resistance to DMS3vir and DMS3vir *acrIF1*, and a lack of newly acquired spacers. Lysogens were determined by broad resistance to both phage and a positive PCR amplification of the c-repressor gene in bacterial genome, amplified using primers 5′-GCGGAATGAGCGCTAAACC-3′ and 5′-CAAGTGCT TTAGCGAGGAATGC-3′. CRISPR resistance was confirmed by resistance to DMS3vir, but not to DMS3vir *acrIF1* and a PCR confirming spacers had been added to one of the CRISPR arrays. Primers 5′-CTAAGCCT TGTACGAAGTCTC-3′ and 5′-CGCCGAAGGCCAGCGCGCCGGTG-3′ were used to amplify CRISPR array 1, and primers 5′-GCCGTCCAGAAGTCA CCACCCG-3′ and 5′-TCAGCAAGTTACGAGACCTCG-3′ for CRISPR array 2. As a positive control for PCR, primers 5′-GCTTGCAGTTCCTCAA CGAG-3′ and 5′CACCAGGAAATTCAGGTAGGG-3′ were used to amplify the housekeeping control gene *fimV*, which encodes a protein that is involved in pilus formation.

Bacterial and phage titres

Bacterial densities were determined by plating on LB agar dilutions of samples taken at each transfer in M9 salts (22 mM Na_2HPO_4; 22 mM KH_2PO_4; 8.6 mM NaCl; 20 mM NH_4Cl; 1 mM $MgSO_4$; and 0.1 mM $CaCl_2$). Phages were extracted at each transfer by chloroform extraction (sample:chloroform 10:1, v/v), and phage titres were determined by spotting serial dilutions of isolated phage samples in M9 salts on a lawn of PA14 Δ*cas7*.

Phage competition

Fixed phenotypes. Competition experiments were performed in glass vials in 6 ml of M9 medium. Experiments were initiated by inoculating a 1:100 dilution of different mixes of overnight cultures of the Δ*cas7* strain and either the surface mutant Δ*pilA*[29] (sm2) or BIM strain (2 spacers targeting DMS3 phage). A 1:1 mix of the phages DMS3vir and DMS3 was added (10^8 PFU) and the vials were incubated at 37 °C with shaking for 8 h. Phages were extracted by chloroform extraction and spot assays carried out to determine phage titre. To determine phage ratios (DMS3:DMS3vir), plaque assays were carried out by serially diluting phage extractions and adding 200 µl of the selected dilution to 600 µl of Δ*cas7* overnight culture and 6 ml molten top agar (0.5%), which was then poured over a prewarmed LB agar plate. The plates were incubated overnight at 37 °C and the plaques generated by temperate and virulent phages were discriminated by differences in opacity, and a subset confirmed by PCR. All experiments were performed in six replicates.

Coevolution competitions. Phage competition was also measured in the presence of host evolution. Initially sensitive Δ*cas7* or wild-type hosts were infected with 10^4 PFU of a 50:50 mix of temperate and virulent phages (DMS3 and DMS3vir). The experiment was run as a standard evolution experiment, and bacterial and phage titres measured every day for seven days. Resistance phenotypes were assessed on days 3 and 7, as described in 'Determination of resistance phenotypes', and plaque assays used to determine the ratio of temperate to virulent phage at each time point.

Competition DMS3 × DMS3 *acrIF*. Temperate DMS3 was also competed against a mutant encoding Acr proteins. Initially sensitive Δ*cas7* or wild-type hosts were infected with 10^4 PFU of a 50:50 mix of DMS3 and DMS3 *acrIF1* (or DMS3 *acrIF4*). The experiment was run for three days and samples of total phage population (that is, free phages + prophages, no chloroform extraction) were collected and immediately frozen every day. Phage titres were measured every day by spot test. To determine their relative fitness, the relative frequencies of each phage were determined at $t = 0$ and at $t = 3$ days by qPCR, following a previously described method[32].

Expression of priming spacers

The expression of the CRISPR RNA encoding spacer 1 of CRISPR2 was restored in strain PA14 ΔCRISPR2 using an arabinose inducible expression vector (pHERD30T-based). In brief, oligonucleotides containing the sequences of a non-targeting (NT) spacer (5′-GTCTTCTTTGAGCTT CCAGAGAACTGAAGAC-3′) or of spacer 1 (5′-ATCAGCCGGACGT TGTAGTAGTCGAGCGCGGT-3′) and flanked by two CRISPR2 repeats were annealed and ligated between NcoI/HindIII restriction sites. The resulting plasmids were transformed into PA14 ΔCRISPR2 to generate the strains ΔCRISPR2-sp1 and ΔCRISPR2-NT, respectively. Similarly, a spacer targeting the natural Pf5 prophage of PA14 (accession number AY324828) with 1 mismatch (bold) 5′-**A**GTCCTTCTAGTGAGCGGAA CCAAAATCTATT-3′ was expressed in the wild-type PA14 strain.

Measuring prophage induction

Single colonies were picked from plated lysogens and grown in LB medium overnight at 37 °C with 180 rpm shaking. The overnight culture

was diluted 1:100 in fresh M9 medium and grown until $OD_{600\,nm}$ reached about 0.1. The cultures were then pelleted by centrifugation and the pellet washed 5 times in M9 buffer, and then resuspended in 10 ml of M9 medium. The cultures were grown at 37 °C with shaking, samples were taken regularly for phage quantification by spot assay and $OD_{600\,nm}$ measurements using the Biotek synergy 2 plate reader.

Twenty-four-hour growth curves

Single colonies were isolated and grown in M9 medium overnight at 37 °C with 180 rpm shaking. The following day, this culture was diluted 1:100 and 250 µl of this mixture was added to a 96-well plate and growth curves were measured for 23 h in a Thermo Scientific Varioskan flash plate reader with continuous shaking at 180 rpm. Readings of $OD_{600\,nm}$ were taken every 15 min and the plate kept at 37 °C. All growth curves were performed in 6–12 replicates.

Bacterial competition

Competition experiments were performed in 6 ml M9 medium supplemented with 0.2% glucose. Competition experiments were initiated by inoculating 1:100 from a 1:1 mixture of overnight cultures (grown in M9 medium + 0.2% glucose) of each strain. If phages were included, they were added at a concentration of 10^4 PFU. Cells were transferred 1:100 daily into fresh broth. At varying time points, from 1 to 7 days, samples were taken and cells were serially diluted in M9 salts and plated on LB agar supplemented with 50 µg ml^{-1} X-gal (to enable discrimination between strains that carry the *lacZ* gene (blue) and those that do not (white)). All experiments were performed in six replicates. Relative fitness was calculated from changes in the relative frequencies of blue and white colonies (relative fitness = [(fraction strain A at $t = x$) × (1 − (fraction stain A at $t = 0$))]/[(fraction strain A at $t = 0$) × (1 − (fraction strain A at $t = x$))]).

Whole-genome sequencing and bioinformatic analyses

Lysogen clones in the Δ*cas7* background and lysogen clones in wild-type and Δ*cas1* backgrounds were isolated from late time points of the evolution experiments. Standard genome sequencing and standard bioinformatic analyses were provided by MicrobesNG (as described at http://www.microbesng.uk). Raw read sequencing data has been deposited in the European Nucleotide Archive under the study accession number PRJEB34503. Trimmed reads were mapped to wild-type PA14 reference genome (accession number NC_008463) with Geneious 9.1.8 software using Bowtie2 mapper[33] to identify the genomic deletion. Reads were also mapped to DMS3 reference genome (accession number DQ631426) and hybrid reads composed of a 5′ extremity deriving from PA14 and a 3′ extremity matching the DMS3 5′ end (and vice versa, read 5′ extremity matching DMS3 3′ end and 3′ extremity deriving from PA14) were extracted. These hybrid reads were then mapped back to PA14 genome to identify prophage insertion sites.

Reporting summary

Further information on research design is available in the Nature Research Reporting Summary linked to this paper.

Data availability

Source Data associated with Figs. 1–4 and Extended Data Figs. 1–3, 5, 7–9 are provided with the paper. Sequencing data have been deposited in the European Nucleotide Archive under the study accession number PRJEB34503. The datasets analysed for the bioinformatic study are available on GitHub at https://github.com/davidchyou/Rollie-Chevallereau.

Code availability

Mathematical algorithms generated during this study are available in the Supplementary Information. Scripts generated for the bioinformatics analyses are available on GitHub at https://github.com/davidchyou/Rollie-Chevallereau.

28. Cady, K. C. & O'Toole, G. A. Non-identity-mediated CRISPR-bacteriophage interaction mediated via the Csy and Cas3 proteins. *J. Bacteriol*. **193**, 3433–3445 (2011).
29. Liberati, N. T. et al. An ordered, nonredundant library of *Pseudomonas aeruginosa* strain PA14 transposon insertion mutants. *Proc. Natl Acad. Sci. USA* **103**, 2833–2838 (2006).
30. Cady, K. C., Bondy-Denomy, J., Heussler, G. E., Davidson, A. R. & O'Toole, G. A. The CRISPR/Cas adaptive immune system of *Pseudomonas aeruginosa* mediates resistance to naturally occurring and engineered phages. *J. Bacteriol*. **194**, 5728–5738 (2012).
31. Ceyssens, P.-J. et al. Comparative analysis of the widespread and conserved PB1-like viruses infecting *Pseudomonas aeruginosa*. *Environ. Microbiol*. **11**, 2874–2883 (2009).
32. Chevallereau, A. et al. Exploitation of the cooperative behaviors of anti-CRISPR phages. *Cell Host Microbe* **27**, 1–10 (2019).
33. Langmead, B. & Salzberg, S. L. Fast gapped-read alignment with Bowtie 2. *Nat. Methods* **9**, 357–359 (2012).
34. Arndt, D. et al. PHASTER: a better, faster version of the PHAST phage search tool. *Nucleic Acids Res*. **44**, W16– W21 (2016).

Acknowledgements We thank A. R. Davidson for providing the mutant strains of PA14 Δ*cas3*, Δ*cas7*, Δ*cas1* and ΔCRISPR2, G. A. O'Toole for the strain CRISPR2 Δsp1–2 and J. Bondy-Denomy for the *Tn::pilA* (*ΔpilA*) PA14 surface mutant. Genome sequencing was provided by MicrobesNG (http://www.microbesng.uk), which is supported by the BBSRC (grant number BB/L024209/1). This work was funded by a grant from the European Research Council (https://erc.europa.eu) (ERC-STG-2016-714478 - EVOIMMECH) and NERC Independent Research Fellowship (NE/M018350/1) awarded to E.R.W. A.C. has received funding from the European Union's Horizon 2020 research and innovation programme under the Marie Skłodowska-Curie grant agreement No 834052. P.C.F. was supported by the Marsden Fund from the Royal Society of New Zealand.

Author contributions Conceptualization of the study was done by C.R., A.C. and E.R.W. Experimental design was carried out by C.R., A.C., B.N.J.W and E.R.W. Bacterial evolution, competition and growth experiments were done by C.R. and A.C. with assistance from O.F. and I.M. Virulent versus temperate phage competitions and prophage induction-rate experiments were performed by C.R. All experiments with acr phages and CRISPR 2 spacer 1 were done by A.C. B.N.J.W. and A.C. carried out Pf5 experiments. The experiment with superinfecting virulent phage was done by E.R.W. C.R., A.C., B.N.J.W., T.-y.C., C.M.B., P.C.F. and E.R.W. analysed the data. S.G. generated theoretical mathematical models. T.-y.C. conducted bioinformatic analyses supervised by C.M.B. and P.C.F. A.C. performed whole-genome sequencing analyses. C.R. wrote the original draft of the manuscript; A.C. wrote the revised version of the manuscript with contributions from C.R., B.N.J.W., T.-y.C., S.G., C.M.B. and P.C.F. E.R.W. supervised the project and provided comments on all versions of the manuscript.

Competing interests The authors declare no competing interests.

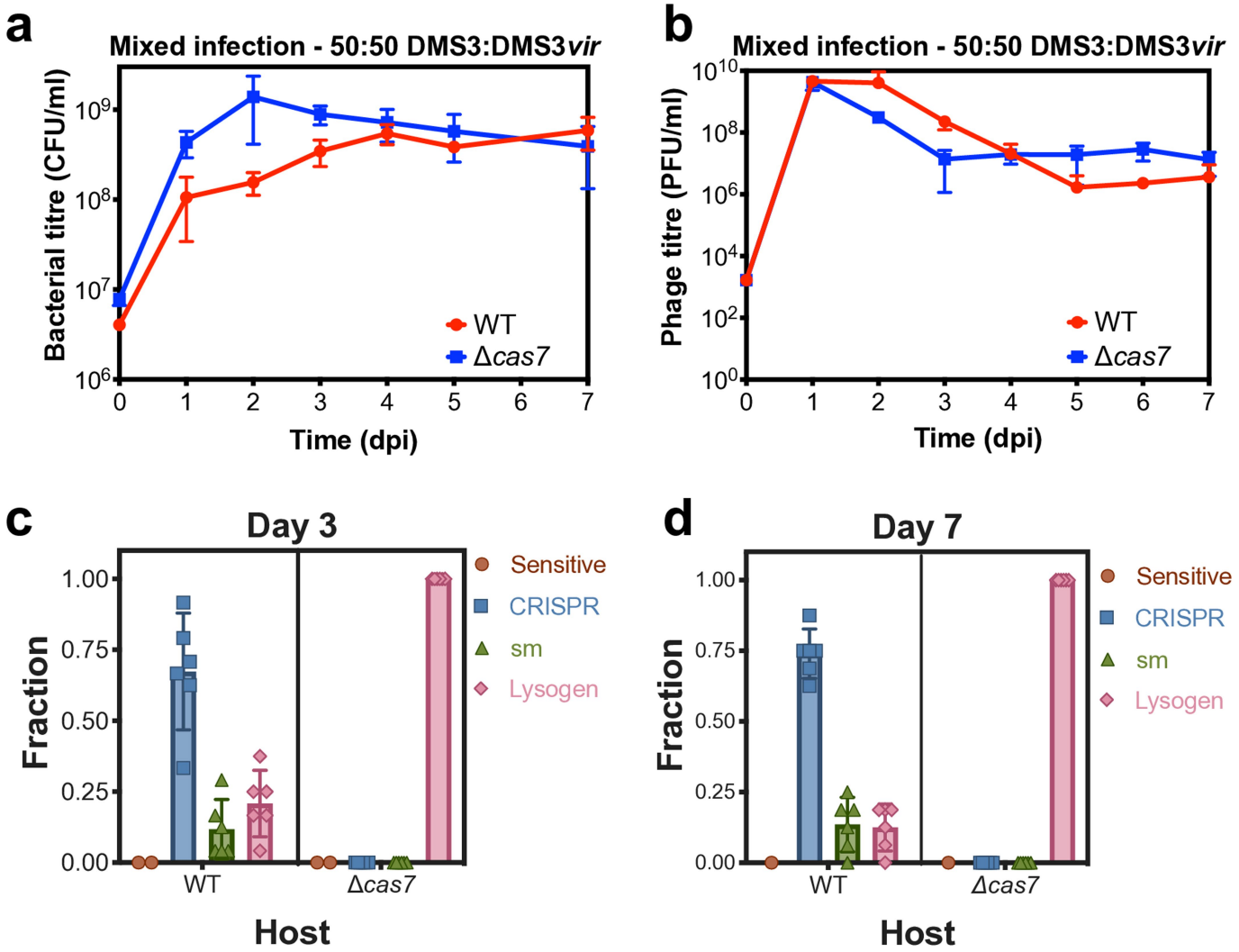
Additional information

Supplementary information is available for this paper at https://doi.org/10.1038/s41586-020-1936-2.

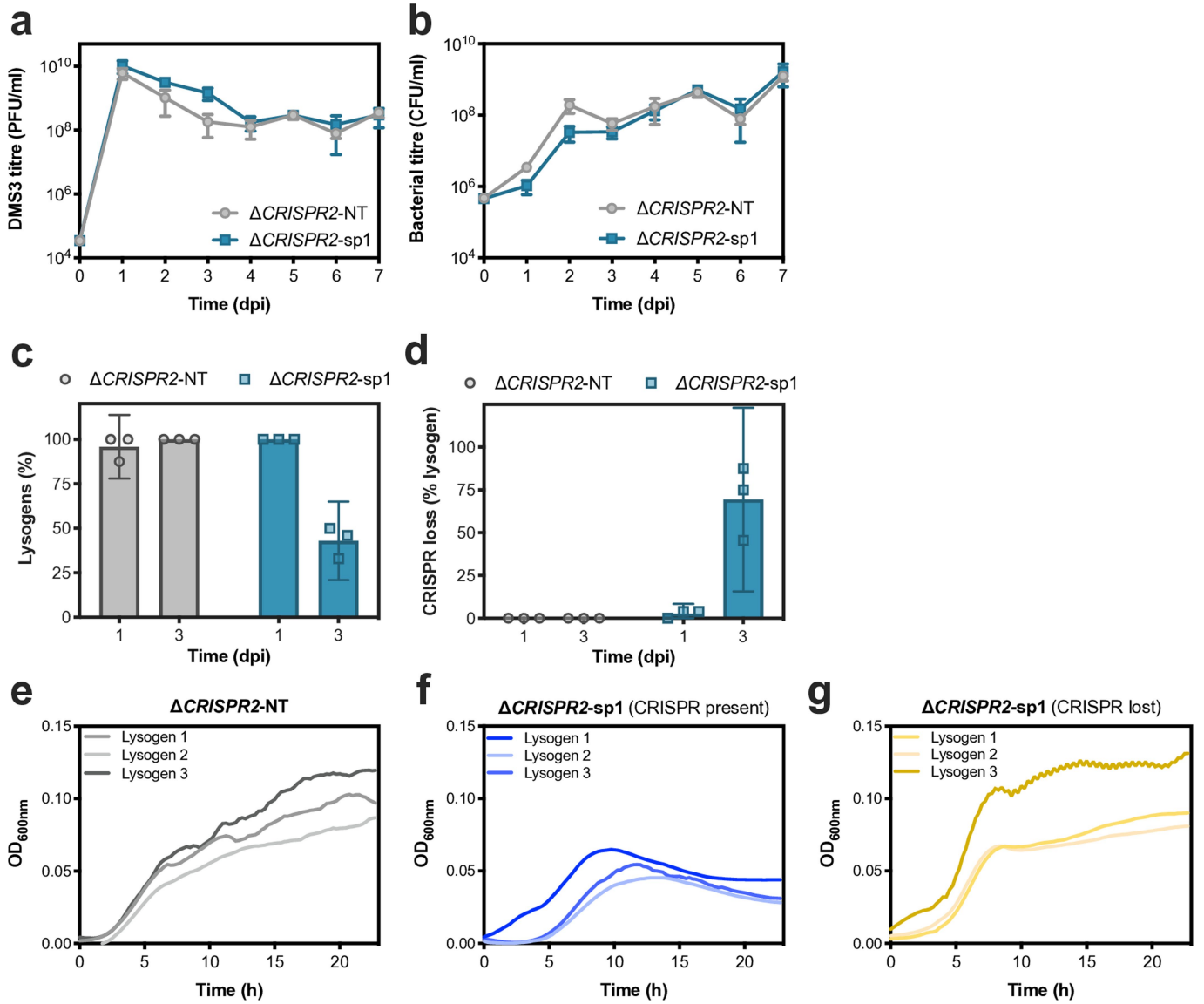
Correspondence and requests for materials should be addressed to C.R., A.C. or E.R.W.

Peer review information *Nature* thanks Eugene Koonin and the other, anonymous, reviewer(s) for their contribution to the peer review of this work.

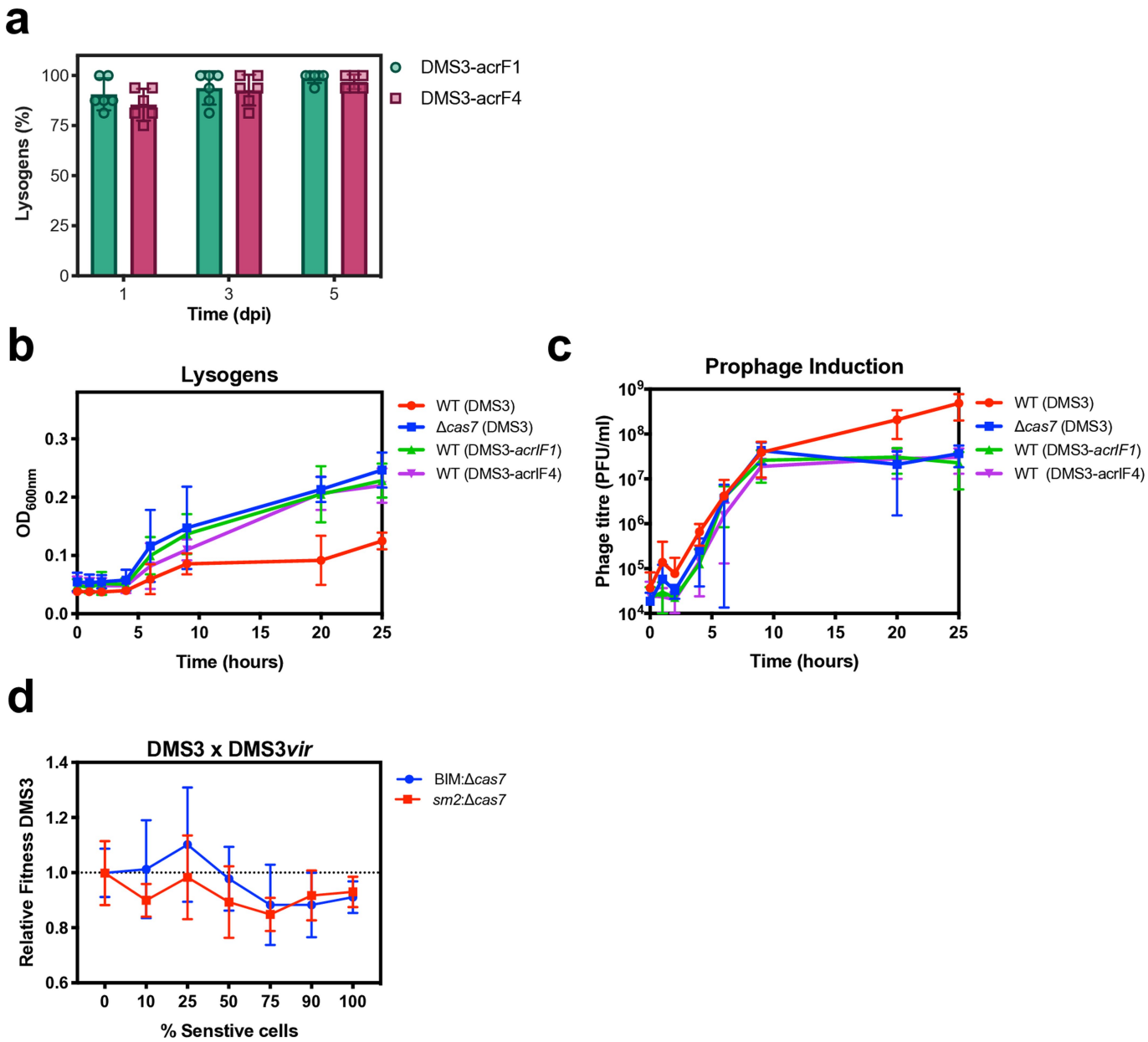
Reprints and permissions information is available at http://www.nature.com/reprints.



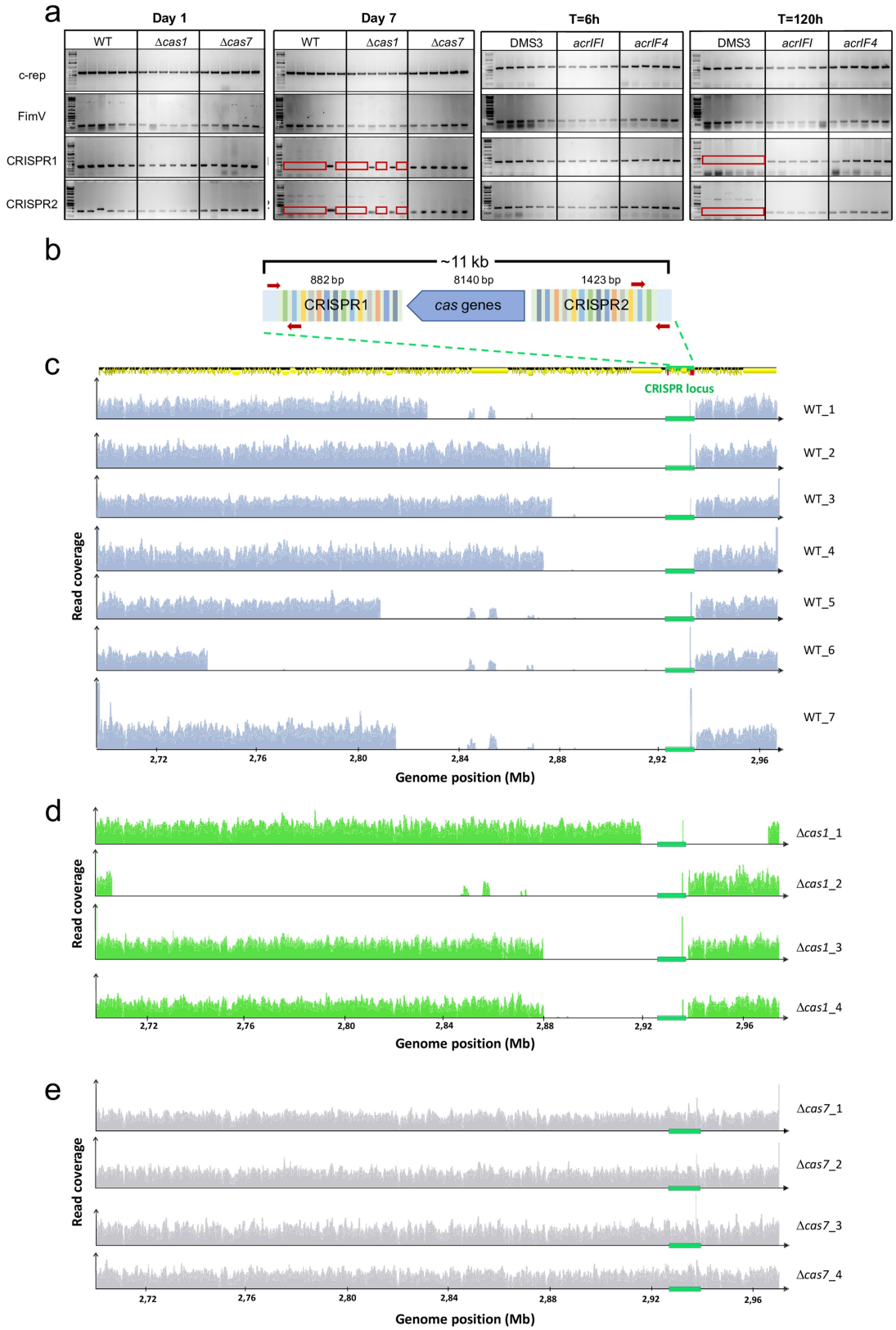
Extended Data Fig. 1 | Infection with a 50:50 mix of temperate:virulent phages. a, **b**, Bacterial (**a**) and phage (**b**) titres during a co-culture experiment of wild-type PA14 (red) or Δ*cas7* mutant (blue), and a 50:50 mix of DMS3 and DMS3vir. **c**, **d**, Resistance phenotypes at day 3 (**c**) or day 7 (**d**) of the co-culture experiment, based on 24 random clones per replicate experiment. Data are the mean of six biological replicates per treatment. Error bars represent 95% confidence intervals.



Extended Data Fig. 2 | The suppression of lysogeny and immunopathological effects are due to spacer 1 of CRISPR array 2. a, **b**, Phage (**a**) and bacterial (**b**) titres during co-culture of phage DMS3 and *P. aeruginosa* PA14 ΔCRISPR2, expressing a non-targeting spacer from a plasmid (ΔCRISPR2-NT) or the original CRISPR2 spacer 1 (ΔCRISPR2-sp1). **c**, **d**,The proportion of lysogens (**c**) and the frequency of loss of CRISPR–Cas immune systems (**d**) at 1 and 3 days post-infection, based on PCR analyses of 24 random clones per replicate experiment. **a**–**d**, Data are the mean of three biological replicates. Error bars represent 95% confidence intervals. **e**–**g**, Growth of three independent lysogen clones isolated at three days post-infection, as determined by $OD_{600\,nm}$ measurements. ΔCRISPR2-NT (**e**) and ΔCRISPR2-sp1 (**f**) lysogen clones carry the ancestral ΔCRISPR2 CRISPR–Cas immune system, whereas the ΔCRISPR2-sp1 (**g**) lysogen clones have evolved to lose CRISPR–Cas.

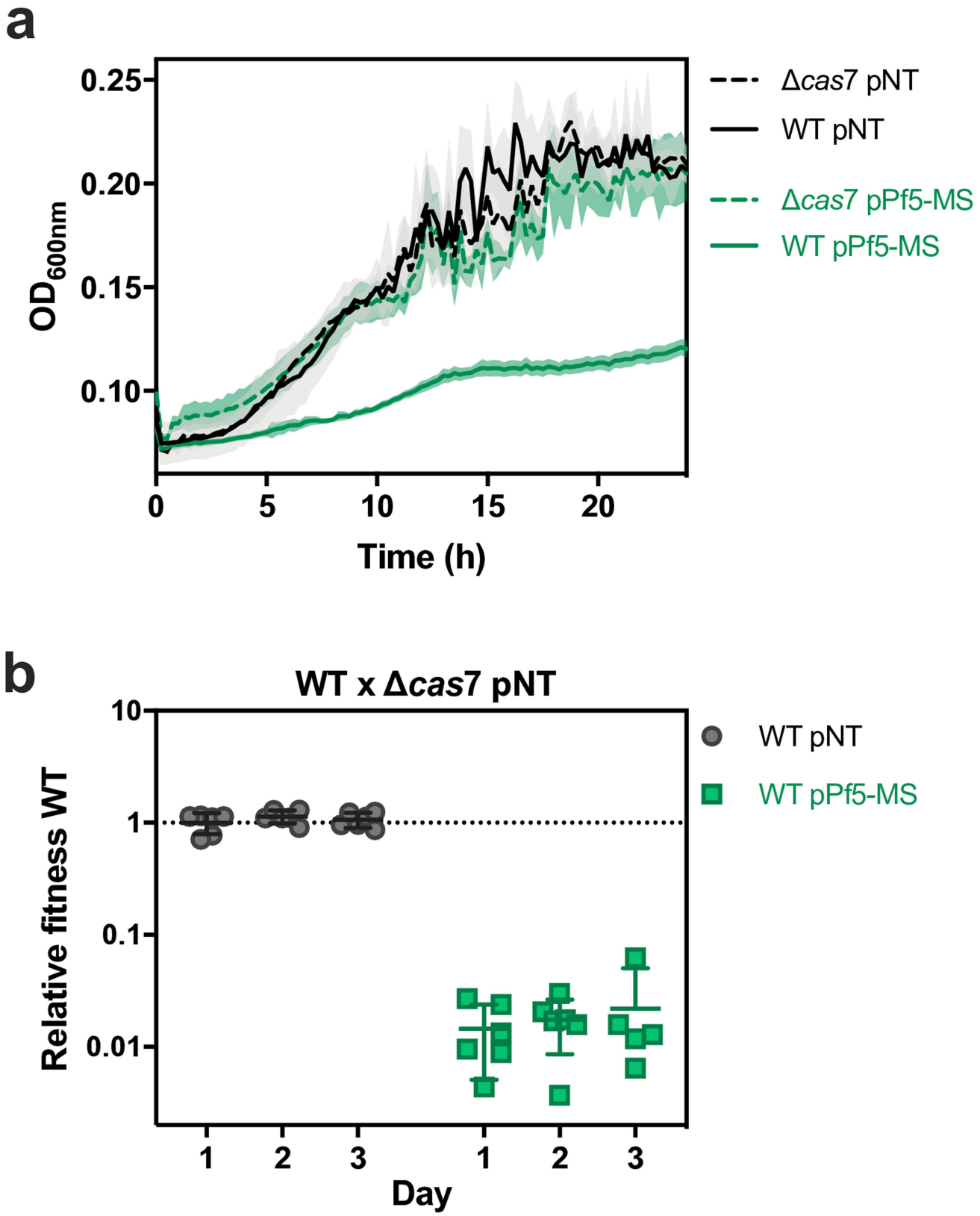


Extended Data Fig. 3 | Prophage induction rates are increased in hosts with active CRISPR–Cas. a, The percentage of lysogens formed upon infection of wild-type host with DMS3 phages engineered to produce AcrIF1 or AcrIF4 anti-CRISPR proteins. **b**, **c**, Optical density (**b**) and phage titres (**c**) during growth of lysogens of DMS3, DMS3 *acrIF1* or DMS3 *acrIF4* phages in a wild-type PA14 or Δ*cas7* genetic background. **d**, Relative fitness of the DMS3 phage during competition with the virulent mutant DMS3vir in the presence of varying fractions of sensitive (Δ*cas7*) host and resistant hosts with CRISPR-based immunity (BIM) or surface-based immunity (sm2) against these phages. Data show mean fitness at 8 h after infection. All panels show the mean of six biological replicates and error bars represent 95% confidence intervals.

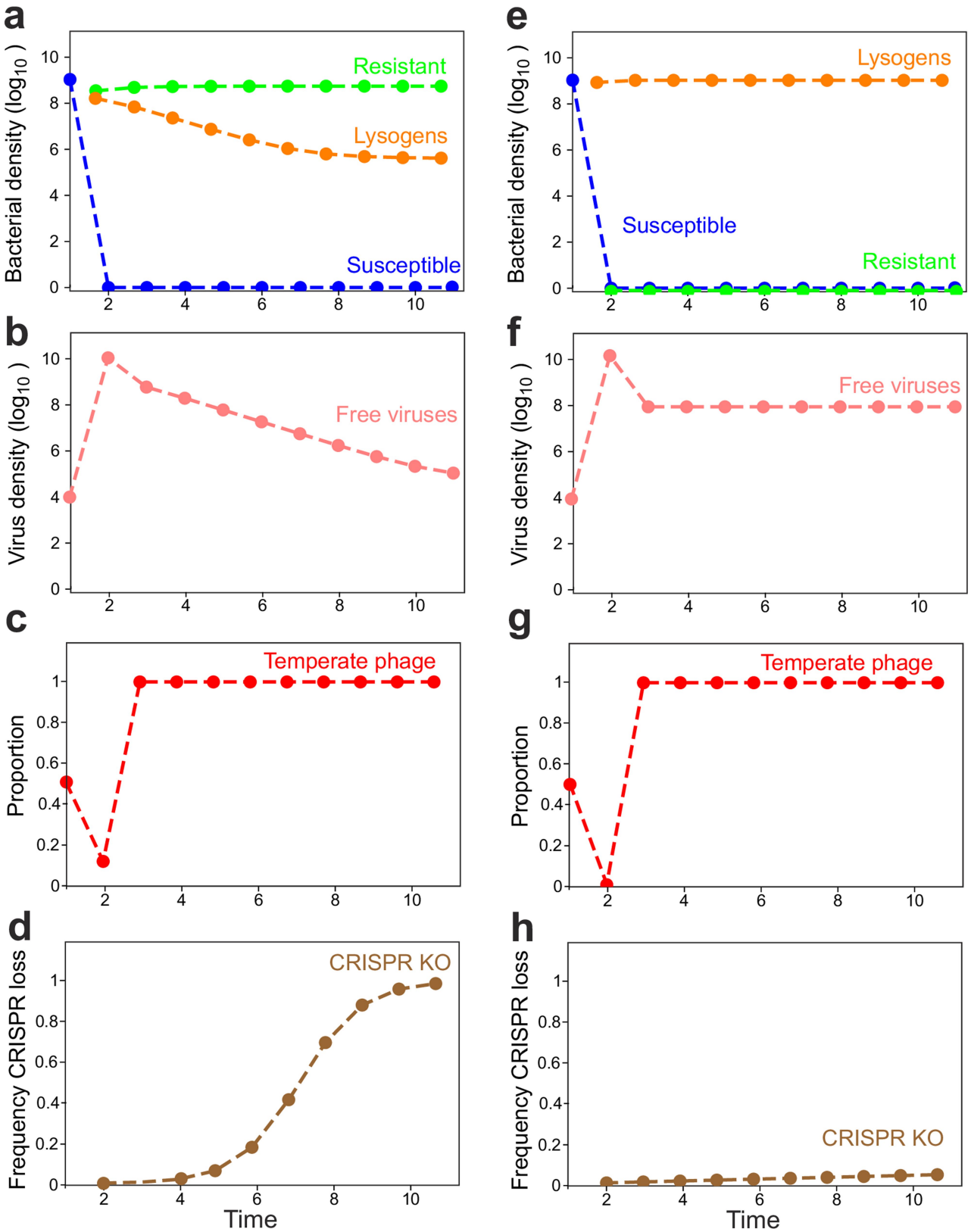


Extended Data Fig. 4 | See next page for caption.

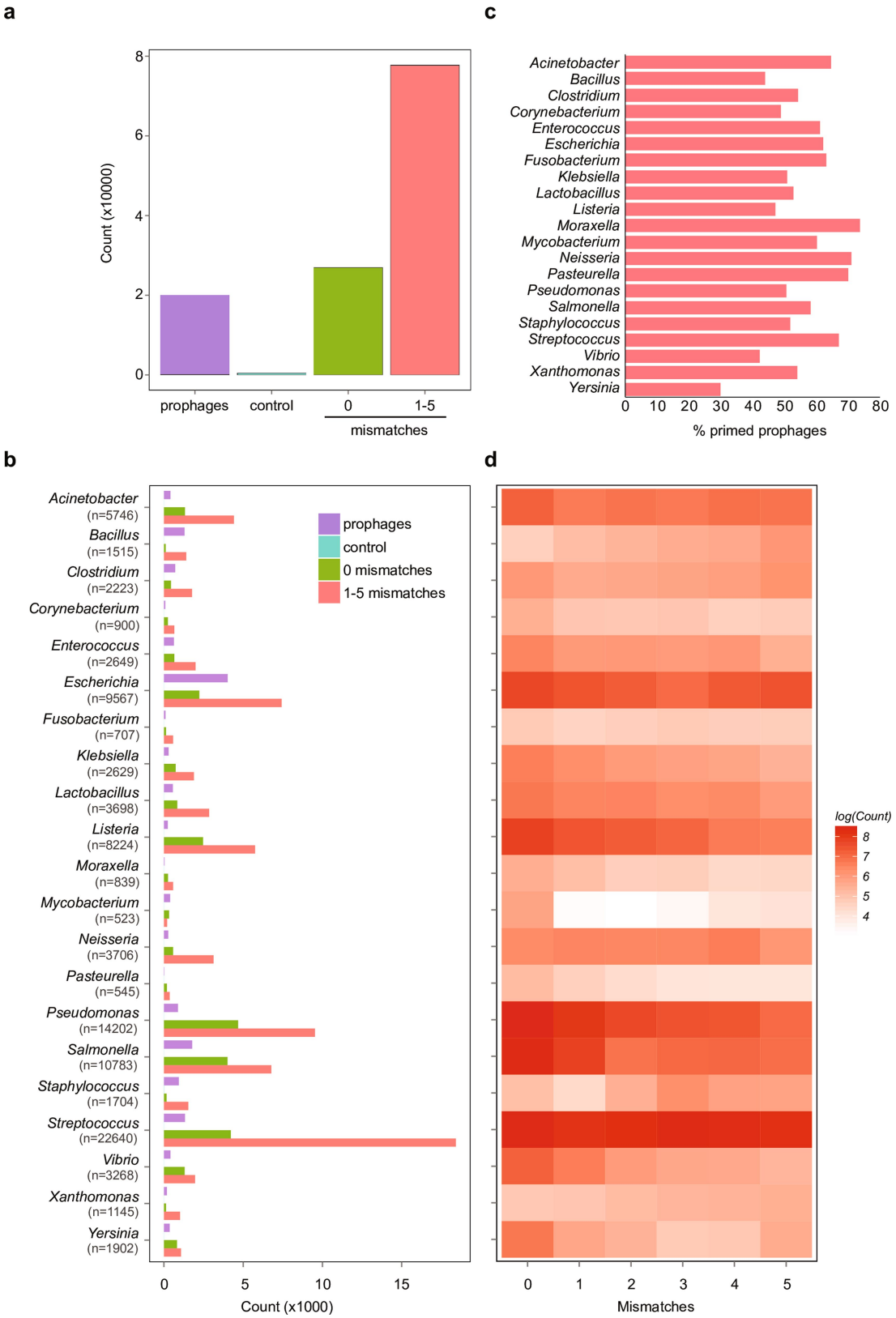
Extended Data Fig. 4 | Lysogens lose their CRISPR–Cas immune systems. **a**, PCR amplification of the c-repressor gene of the prophage (*c-rep*, 611 bp), the *fimV* gene (located about 1 Mb from the CRISPR loci and used as a positive control for the PCR, 116 bp) and CRISPR loci 1 (349 bp) and 2 (206 bp) on the host genome. PCRs were performed on 6 independent DMS3 lysogens in wild-type, Δ*cas1* and Δ*cas7* backgrounds isolated at 1 or 7 days post-infection, as well as on 6 independent lysogens of DMS3, DMS3 *acrIF1* or DMS3 *acrIF4* (wild-type background) isolated at 6 or 120 h after infection. Red frames indicate a failure to amplify a product. PCR amplifications were performed on clones isolated from three biological replicate experiments and produced similar results. For gel source data, see Supplementary Fig. 1. **b**, Schematic of the CRISPR–Cas locus of wild-type PA14, which spans a region of around 11 kb. Primers used to amplify regions of CRISPR arrays 1 or 2 are shown as red arrows. **c**–**e**, Whole-genome sequencing of DMS3 lysogens that lost their CRISPR–Cas system (red frames in **a**) in wild-type PA14 (**c**), Δ*cas1* (**d**) or Δ*cas7* (**e**) backgrounds. Graphs show the read coverage of the region encompassing positions 2.70–2.97 Mb of the wild-type PA14 genome. The CRISPR–Cas locus is indicated by a green box on the *x* axis. A genome map depicting coding sequences (yellow arrows) is shown above the graphs. The region comprising 2.84–2.88 Mb includes sequences that are repeated elsewhere on the PA14 genome, explaining why reads that map to these positions are still detected in some of the deletion mutants. The high peak at the 3′ end of the CRISPR locus corresponds to the coverage of spacer 20 of CRISPR2 by reads that derive from DMS3 prophage (5′ and 3′ extremities of these reads map to the phage genome). Spacer 20 of CRISPR2 has 100% identity to DMS3 but is not immunogenic because there is no consensus protospacer-adjacent motif.



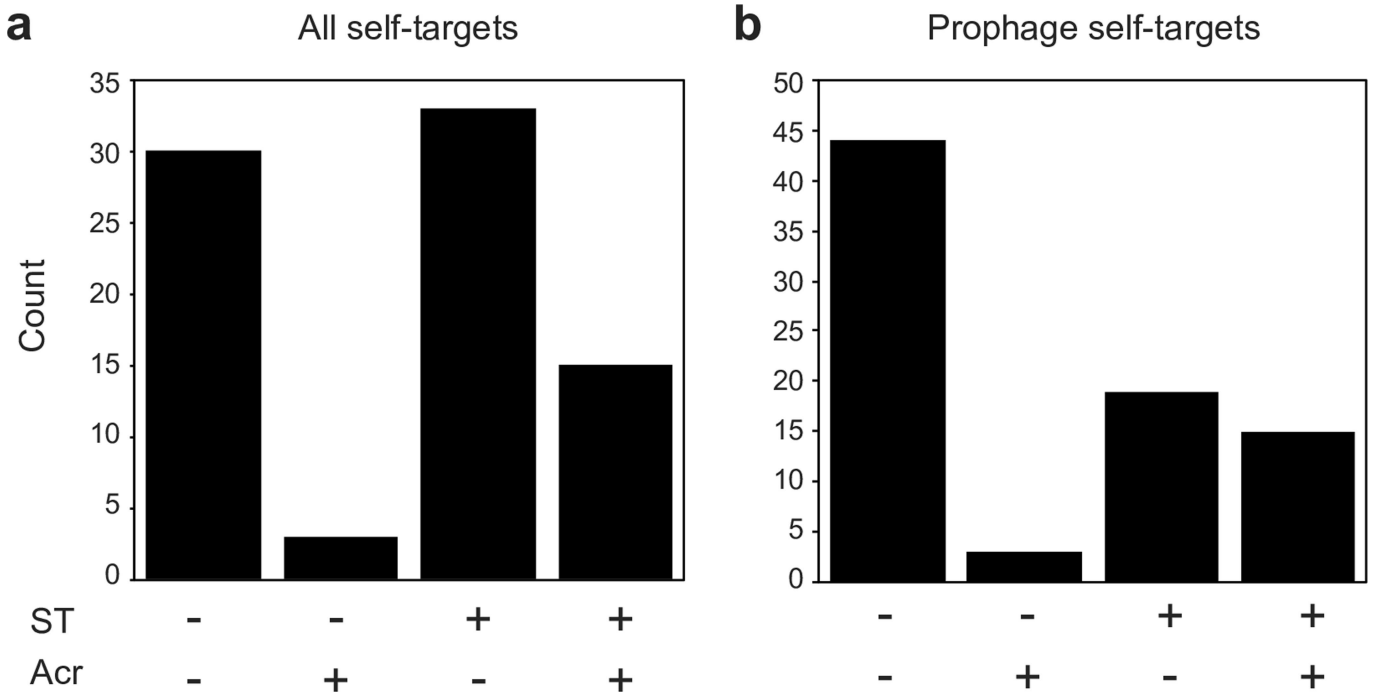
Extended Data Fig. 5 | Expression of Pf5 priming spacer in *P. aeruginosa* PA14. a, Growth of Δ*cas7* (dashed line) or wild-type (solid line) clones carrying an expression plasmid encoding a non-targeting spacer (pNT) or a spacer targeting the PA14 natural prophage Pf5 with one mismatch (pPf5-MS), as determined by $OD_{600\,nm}$ measurements. Graphs show mean curves from 6 biological replicates, and shaded areas correspond to 95% confidence intervals. **b**, Relative fitness of wild-type pNT or wild-type pPf5-MS during competition with Δ*cas7* pNT. Data are the mean of six biological replicates per treatment. Error bars represent 95% confidence intervals.



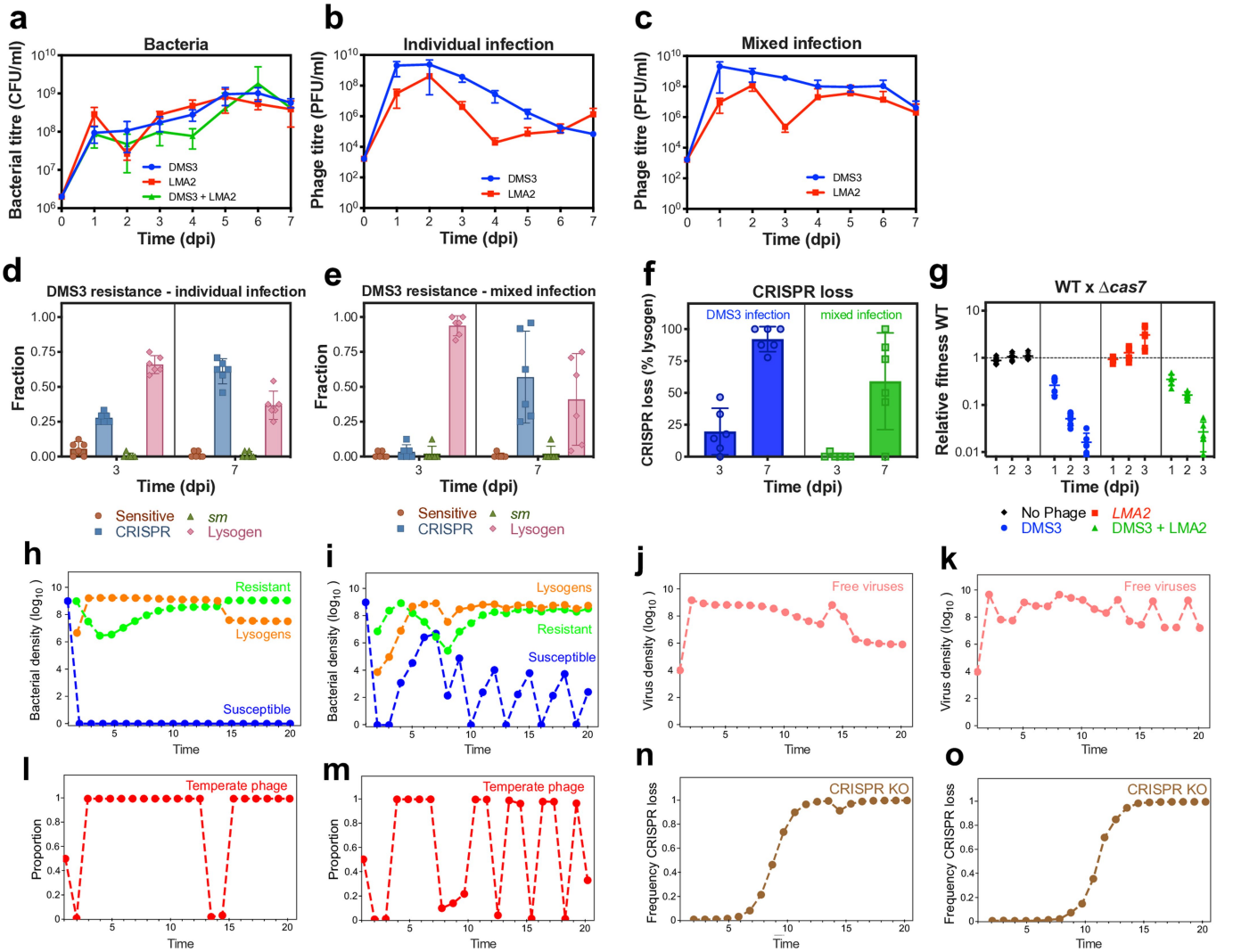
Extended Data Fig. 6 | Simulations of population and evolutionary dynamics of bacteria–phage interactions, when virulent and temperate phages compete on bacteria with a CRISPR–Cas system. a–**c**, **e**–**g**, Graphs show densities of susceptible hosts, CRISPR-resistant bacteria and lysogens (**a**, **e**) or free viruses over time (**b**, **f**), as well as the proportion of temperate phages in a population composed of both temperate and virulent types (**c**, **g**). Temperate phages can transmit both horizontally and vertically, whereas virulent phages can transmit only horizontally and cannot superinfect lysogens. **d**, **h**, Frequency of evolutionary loss of CRISPR–Cas system in the lysogen population over time. The simulations shown in **a**–**d** reflect a situation in which both virulent and temperate phages lack acr genes, whereas those in **e**–**h** reflect a scenario in which the temperate type carries an acr gene.



Extended Data Fig. 7 | Matches between spacers and temperate phages are widespread. a, Total matches between non-redundant spacers (n = 1,239,973) from 171,361 RefSeq and GenBank complete genomes and a non-redundant set of temperate phages (n = 19,996)[21]. The counts of perfect (0) or mismatched (1–5) targets are shown. As a control, the temperate phages were shuffled ten times, while retaining the hexanucleotide content (control). **b**, Counts of spacers matching temperate phages from all genera with over 500 spacer–prophage matches. The total number (n) of spacer–prophage matches is shown for each genus in parentheses. Counts of matches are shown (0, green; 1–5 mismatches, red). The number of temperate phages analysed is plotted (prophages in purple) as are the matches to shuffled prophages. The control is shown in blue, but is not visible because it had only 0 to 10 counts. **c**, The percentage of prophages within each genus that were targeted by self-priming spacers (1–5 mismatches). **d**, Heat map of the distribution of mismatches (0–5). Genera are as in **b** and data are shown as log(count) for each genus, as the number of matches varied widely between genera.



Extended Data Fig. 8 | Self-targeting genomes are enriched for acr gene(s). **a**, **b**, The number of *P. aeruginosa* genomes with complete CRISPR–Cas systems that contain (+) or lack (–) genes encoding known Acr proteins. For these strains, the total number of strains with perfect (0) or mismatched (1–5) self-targeting (ST) spacers to anywhere in the genome (**a**) or to prophages (**b**) are shown. For complete *P. aeruginosa* genomes, all self-targeting events were analysed for matches to prophages using PHASTER[34]. The number of genomes with acr genes (acr +) and self-targeting (ST +) spacers is significantly greater than the number of genomes with acr genes and without self-targeting spacers ($P = 8.14 \times 10^{-5}$, two-sided Fisher's exact test, $n = 71$).



Extended Data Fig. 9 | Presence of a superinfecting virulent phage does not alter immunopathological effects. a–**c**, Bacterial (**a**) and phage titres upon individual (**b**) or mixed (**c**) infection of wild-type PA14 with phage DMS3 and virulent phage LMA2. **d**, **e**, Resistance phenotypes evolved by bacteria against DMS3 upon individual (**d**) or mixed (**e**) infection. **f**, Frequency of loss of CRISPR–Cas immune systems upon infection with phage DMS3 or with both the phages DMS3 and LMA2, based on 24 random clones per replicate experiment. **g**, Relative fitness of wild-type PA14 during competition with PA14 Δ*cas7* in the presence or absence of phages DMS3 and LMA2. **a**–**g**, Data are the means of six biological replicates. Error bars indicate 95% confidence intervals. **h**–**o**, Simulations of population and evolutionary dynamics during infection of bacteria carrying CRISPR–Cas systems with a mixed population of unrelated virulent and temperate phages. Graphs show densities of susceptible hosts, CRISPR-resistant bacteria and lysogens (**h**, **i**) and free viruses over time (**j**, **k**), as well as the frequencies of temperate phages in a population composed of both temperate and virulent types (**l**, **m**). Temperate phage can transmit both horizontally and vertically, whereas virulent phage can transmit only horizontally and can superinfect the lysogens (because temperate and virulent phages are unrelated). **n**, **o**, Frequencies of evolutionary loss of CRISPR–Cas system in the lysogen population over time. The simulations shown in **h**, **j**, **l**, **n** reflect a scenario in which bacteria can evolve CRISPR-based resistance against both phages, whereas those shown in **i**, **k**, **m**, **o** reflect a situation in which CRISPR-based resistance does not evolve against the virulent phage, and bacteria instead evolve costly surface-based resistance (as it is the case in our experiments). A detailed description of the simulations is provided in the Supplementary Information.

Extended Data Table 1 | Genomic deletions and prophage insertion sites in DMS3 late lysogen clones

Strain	Sample name	Name on ED Fig. 4	Deleted region			Prophage insertion site(s)	
			Start (bp)	End (bp)	Length (bp)	Position (bp)	Proportion of mapped hybrid reads[a]
PA14 WT	WT117	WT_1	2,831,115	2,938,245	**107,131**	replace deleted region	73
	WT221	WT_2	2,879,871	2,938,280	**58,410**	replace deleted region	44.2
						3,555,252	42.3
	WT3213	WT_3	2,880,477	2,938,285	**57,809**	replace deleted region	84
	WT4313	WT_4	2,878,050	2,938,509	**60,460**	replace deleted region	72.3
						3,944,997	6.3
						4,067,332	3.8
						4,453,953	2.5
	WT566[b]	-	0	0	**0**	nd	nd
	WT6615	WT_5	2,812,027	2,938,165	**126,139**	replace deleted region	42.0
						3,325,229	49.6
	WT7AnneD1	WT_6	2,743,638	2,938,176	**194,539**	replace deleted region	22.6
						5,214,542	28.9
						5,732,030	24.0
						5,860,538	22.6
	WT8AnneD2	WT_7	2,818,271	2,938,290	**120,020**	2,335,454	24.8
						2,652,167	29.6
						replace deleted region	21.8
						3,079,052	21.3
PA14 Δ*cas1*	cas11114	Δ*cas1*_1	2,918,943	2,970,427	**51,485**	3,079,190	84.3
	cas1222	Δ*cas1*_2	2,706,504	2,938,538	**232,035**	replace deleted region	90.6
						4,478,625	2.8
	cas1333[c]	-	0	0	**0**	partial	nd
	cas14415	Δ*cas1*_3	2,879,882	2,938,523	**58,642**	2,730,814	44.1
						replace deleted region	46.0
						4,481,869	3.1
	cas1555[d]	-	2,902,848	2,938,280	**35,433**	replace deleted region	78.8
						2,934,176	7.7
	cas16611	Δ*cas1*_4	2,879,874	2,938,285	**58,412**	replace deleted region	94.2
PA14 Δ*cas7*	cas7114	Δ*cas7*_1	0	0	**0**	1,120,809	86.7
	cas72211	Δ*cas7*_2	0	0	**0**	410,059	82.9
	cas73313	Δ*cas7*_3	0	0	**0**	5,725,887	74.7
	cas7442	Δ*cas7*_4	0	0	**0**	5,743,045	84.5
	cas7554	-	0	0	**0**	905,180	37.9
	cas7669	-	0	0	**0**	1,667,097	75.0

[a]The sum does not reach 100% because a proportion of hybrid reads that mapped to the PA14 genome did not enable the identification of a potential prophage insertion site.
[b]Sample was contaminated with a BIM clone; sequencing data are not interpretable.
[c]Only 2,607 bp of DMS3 DNA (including the c-repressor gene) are inserted in bacterial genome at position 5,834,730.
[d]A mixed population, in which reads matching the CRISPR locus are still detectable but coverage is very low.

nature research

Corresponding author(s): Anne Chevallereau, Edze Westra, Clare Rollie

Last updated by author(s): 07/11/2019

Reporting Summary

Nature Research wishes to improve the reproducibility of the work that we publish. This form provides structure for consistency and transparency in reporting. For further information on Nature Research policies, see Authors & Referees and the Editorial Policy Checklist.

Statistics

For all statistical analyses, confirm that the following items are present in the figure legend, table legend, main text, or Methods section.

n/a	Confirmed	
☐	☒	The exact sample size (*n*) for each experimental group/condition, given as a discrete number and unit of measurement
☐	☒	A statement on whether measurements were taken from distinct samples or whether the same sample was measured repeatedly
☐	☒	The statistical test(s) used AND whether they are one- or two-sided *Only common tests should be described solely by name; describe more complex techniques in the Methods section.*
☒	☐	A description of all covariates tested
☐	☒	A description of any assumptions or corrections, such as tests of normality and adjustment for multiple comparisons
☐	☒	A full description of the statistical parameters including central tendency (e.g. means) or other basic estimates (e.g. regression coefficient) AND variation (e.g. standard deviation) or associated estimates of uncertainty (e.g. confidence intervals)
☐	☒	For null hypothesis testing, the test statistic (e.g. *F*, *t*, *r*) with confidence intervals, effect sizes, degrees of freedom and *P* value noted *Give P values as exact values whenever suitable.*
☒	☐	For Bayesian analysis, information on the choice of priors and Markov chain Monte Carlo settings
☒	☐	For hierarchical and complex designs, identification of the appropriate level for tests and full reporting of outcomes
☒	☐	Estimates of effect sizes (e.g. Cohen's *d*, Pearson's *r*), indicating how they were calculated

Our web collection on statistics for biologists contains articles on many of the points above.

Software and code

Policy information about availability of computer code

Data collection	No software was used for data collection
Data analysis	Data analysis and figures were made in R version 3.5.1. or Graphpad Prism 7. Whole-genome sequences analyses were done in Geneious® 9.1.8 software using Bowtie2 mapper. Custom scripts used in bioinformatics analyses are available on github at https://github.com/davidchyou/Rollie-Chevallereau

For manuscripts utilizing custom algorithms or software that are central to the research but not yet described in published literature, software must be made available to editors/reviewers. We strongly encourage code deposition in a community repository (e.g. GitHub). See the Nature Research guidelines for submitting code & software for further information.

Data

Policy information about availability of data

All manuscripts must include a data availability statement. This statement should provide the following information, where applicable:

- Accession codes, unique identifiers, or web links for publicly available datasets
- A list of figures that have associated raw data
- A description of any restrictions on data availability

Source data associated with main figures and Extended Data Figures 1,2,3,5,7,8 and 9 are available in the online version of this publication. Sequencing data have been deposited in the European Nucleotide Archive under the study accession number PRJEB34503. The datasets analysed for the bioinformatic study are available on github at https://github.com/davidchyou/Rollie-Chevallereau

Field-specific reporting

Please select the one below that is the best fit for your research. If you are not sure, read the appropriate sections before making your selection.

☒ Life sciences ☐ Behavioural & social sciences ☐ Ecological, evolutionary & environmental sciences

For a reference copy of the document with all sections, see nature.com/documents/nr-reporting-summary-flat.pdf

Life sciences study design

All studies must disclose on these points even when the disclosure is negative.

Sample size	All experiments were performed in 6 independent biological replicates for sufficient statistical power, in line with common practice in experimental evolution studies.
Data exclusions	No data were excluded
Replication	We used 6 independent biological replicates per treatment. All observations were reproducible.
Randomization	Not relevant to our study - single experimental manipulations of individual variables.
Blinding	Blinding not relevant - single experimental manipulations of individual variables.

Reporting for specific materials, systems and methods

We require information from authors about some types of materials, experimental systems and methods used in many studies. Here, indicate whether each material, system or method listed is relevant to your study. If you are not sure if a list item applies to your research, read the appropriate section before selecting a response.

Materials & experimental systems

n/a	Involved in the study
☒	☐ Antibodies
☒	☐ Eukaryotic cell lines
☒	☐ Palaeontology
☒	☐ Animals and other organisms
☒	☐ Human research participants
☒	☐ Clinical data

Methods

n/a	Involved in the study
☒	☐ ChIP-seq
☒	☐ Flow cytometry
☒	☐ MRI-based neuroimaging